IEEE Access
Multidisciplinary | Rapid Review | Open Access Journal

Received 3 April 2023, accepted 20 April 2023, date of publication 24 April 2023, date of current version 3 May 2023.

Digital Object Identifier 10.1109/ACCESS.2023.3270102

RESEARCH ARTICLE

Motion Analysis Using Global Navigation Satellite System and Physiological Data

ALEŠ PROCHÁZKA[1,2], (Life Senior Member, IEEE), ALEXANDRA MOLČANOVÁ[1], HANA CHARVÁTOVÁ[3], OANA GEMAN[4], (Senior Member, IEEE), AND OLDŘICH VYŠATA[5], (Member, IEEE)

[1]Department of Mathematics, Informatics and Cybernetics, University of Chemistry and Technology Prague, 160 00 Prague, Czech Republic
[2]Czech Institute of Informatics, Robotics and Cybernetics, Czech Technical University in Prague, 160 00 Prague, Czech Republic
[3]Faculty of Applied Informatics, Tomas Bata University in Zlín, 760 01 Zlín, Czech Republic
[4]Department of Health and Human Development, Stefan cel Mare University of Suceava, 720229 Suceava, Romania
[5]Department of Neurology, Faculty of Medicine in Hradec Králové, Charles University, 500 05 Hradec Králové, Czech Republic

Corresponding author: Aleš Procházka (A.Prochazka@ieee.org)

This work involved human subjects or animals in its research. Approval of all ethical and experimental procedures and protocols was granted by the Ethics committee of the Neurological Center at Rychnov n. Kn., Czech Republic.

ABSTRACT Motion analysis using wearable sensors is an essential research topic with broad mathematical foundations and applications in various areas, including engineering, robotics, and neurology. This paper presents the use of the global navigation satellite system (GNSS) for detecting and recording the position of a moving body, along with signals from additional sensors, for monitoring of physical activity and analyzing heart rate dynamics during running on route segments of different slopes and speeds. This method provides an alternative to the heart monitoring on the treadmill ergometer in the cardiology laboratory. The proposed computational methodology involves digital data preprocessing, time synchronization, and data resampling to enable their correlation, feature extraction both in time and frequency domains, and classification. The datasets include signals acquired during ten experimental runs in the selected area. The motion patterns detection involves segmenting the signals by analysing the GNSS data, evaluating the patterns, and classifying the motion signals under different terrain conditions. This classification method compares neural networks, support vector machine, Bayesian, and k-nearest neighbour methods. The highest accuracy of 93.3 % was achieved by using combined features and a two-layer neural network for classification into three classes with different slopes. The proposed method and graphical user interface demonstrate the efficiency of multi-channel and multi-dimensional signal processing with applications in rehabilitation, fitness movement monitoring, neurology, cardiology, engineering, and robotic systems.

INDEX TERMS Multichannel signal processing, global navigation satellite systems, feature extraction, machine learning, computational intelligence, classification, physical activity monitoring, cardiology.

I. INTRODUCTION

Analysis of motion forms a very important research area with applications in engineering, robotics, biomedicine, cardiology, and neurology [1], [2], [3], [4], [5], among others. The rapid progress of related topics is closely linked to the availability of the Global Positioning System (GPS) for general use, which began in the early 1990s, and the ability to determine position coordinates. This has opened up new applications in navigation, transport, geodesy, and motion monitoring in physical activities and sports [6], [7]. The use of these systems has been associated with the rapid technological progress of specific sensor systems, smartphones [8], [9], [10], [11], and smartwatches [12]. The present paper is devoted to this topic, with applications to the analysis of physical activities [13], [14], which is important for detecting motion disorders [15], health monitoring [16], [17], [18], [19], rehabilitation, and for the study oh heart dynamics as well.

The associate editor coordinating the review of this manuscript and approving it for publication was Jiafeng Xie.

Wearable sensors are versatile devices with a wide range of applications. Figure 1 illustrates the approximate timeline of sensors that have been implemented in smartphones over the last 30 years, demonstrating the rapid technological progress of wearable devices [16]. These devices enable monitoring of motion, environmental data, and physiological signals. The data collected by these sensors have a wide range of diverse applications in engineering and biomedicine.

There are several systems taking advantage of GNSS systems for motion monitoring. Mobile devices are usually equipped with sensors which are able to cooperate with the majority of them, including [20], [21] the American GPS system, the European Galileo, the Russian Glonass, and the Chinese BeiDou, among others. Uncorrected GNSS systems using basic information directly from satellites can be quite imprecise, with an accuracy of several meters. The use of this system requires the use of signals from at least four satellites. Three of them provide information about the location and the fourth one serves as a clock bias which provides the difference in time between the receiver's system time and the satellites' system time. Figure 2 presents the principle for locating an object using a set of satellites on the Earth's orbit and the GNSS handset.

More sophisticated systems use a real-time kinematic system (RTK) for precise geolocation [22], [23] and the GNSS reference receiver, to increase the precision of the observation. Mobile phones, on the other hand, typically use GNSS SPP (Single Point Positioning) or Assisted GNSS (A-GNSS) techniques for location-based services. These techniques do not require a reference receiver as they rely on signals from GNSS satellites and network-based assistance data, respectively. The newest dual band GNSS provide another option for increasing the accuracy and correcting for atmospheric effects.

The unifying background of motion analysis is formed by a similar mathematical background that includes general methods of digital signal analysis and processing [24], [25], optimization methods, computational intelligence, and the use of machine learning. Associated methods include functional transforms, time–frequency, and time-scale signal analysis, using the discrete Fourier and wavelet transforms.

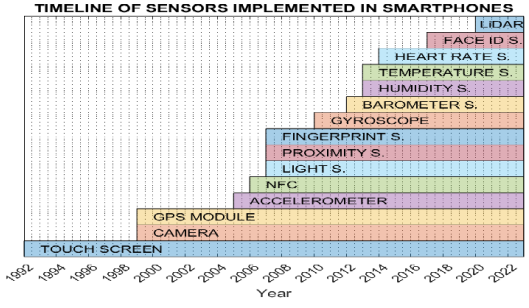

FIGURE 1. Approximate timeline of sensors implemented in smartphones during the last 30 years showing the rapid technological progress of wearable instruments.

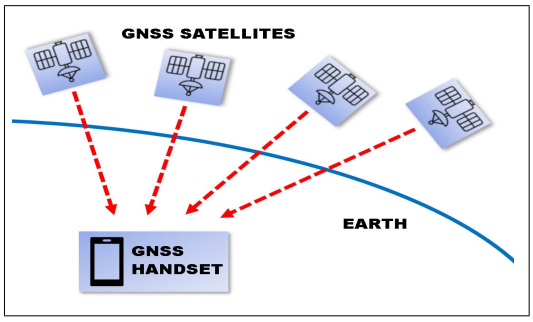

FIGURE 2. Principle of locating an object using a set of satellites on the Earth's orbit and a GNSS handset.

Special methods include image processing and detection of image components using image, depth, and thermal sensors.

This paper presents the use of the global navigation satellite system (GNSS) [20], [21], [26], [27] for detecting and recording the position of a moving body [28] during monitoring of physical activity and the simultaneous acquisition of signals from biosensors and accelerometers [29], [30], [31], [32]. Figure 3 presents the route recorded by the GNSS system, its location above the mapping background, and satellite and physiological signals acquired. Figure 3(c) presents the altitude profile and changes of the running speed for the whole route acquired by the GNSS system and presented in Fig. 3(b). Figures 3(d,e) present accelerometric and heart rate signals recorded during the run for a selected experiment.

The project has the following objectives: (i) to explore the use of mobile sensors for monitoring physical activities, (ii) to propose the use of computational intelligence for data processing, and (iii) to detect possible heart disorders during different loads in the natural environment. The results obtained during natural runs provide additional information to the data acquired in a cardiology laboratory using the treadmill ergometer [33], [34], which allows for changes in speed and slope during each exercise. The paper shows how these conditions of data acquisition in the natural environment can be estimated by the GNSS data recorded by sensors in the mobile phone. Further, closely related studies [35] are devoted to the use of wearable photoplethysmographic sensors during treadmill exercises and in natural conditions.

The proposed method is based upon the analysis of the signals acquired in real physical conditions from the set of experiments. Selected data features and machine learning methods are used to find a computational system for the evaluation of the patterns of motion under different conditions. This approach is applied to real signals but with the possible use of similar methods in virtual systems [36], [37] based on augmented reality and trainers working on virtual reality platforms allowing motion activities and analysis in conditions very close to real ones.

II. METHODS

The whole dataset includes data recorded by wearable sensors in a smartphone (the three-axis accelerometer and GNSS receiver recording terrestrial data of longitude, latitude,

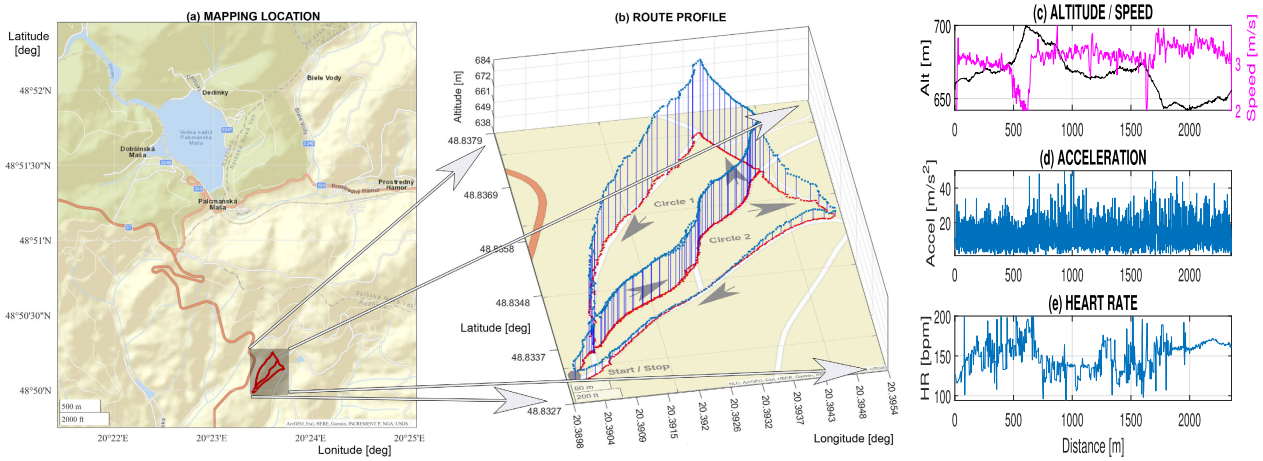

FIGURE 3. Route details presenting (a) the location of the experimental trajectory acquired by the Matlab mapping toolbox, (b) the detailed route and its profile recorded by the GNSS system above the mapping background with the starting/ending point, and (c,d,e) signals acquired during a selected experiment.

and altitude), and the heart rate sensor (paired with the smartwatch). These procedures involving human participants were in accordance with the ethical standards of the institutional research committee and with the 1964 Helsinki Declaration and its later amendments.

The experiments include 10 runs in real conditions along the route, with segments of the different slopes. Detailed descriptions of each observation are contained at the IEEE DataPort (doi: https://dx.doi.org/10.21227/759s-8s08) for further investigation. This repository includes the terrestrial and physiological data acquired during all experiments, the Matlab graphical user interface, and a graphical video abstract of the paper.

A. GNSS DATA PROCESSING

Since the datasets were recorded always on the same route, there was a requirement for the evaluation of the average route from all GNSS records. This task was not easy to carry out because of the fact that there was no quantity which was constant for a specific point on the route throughout all measurements. The time elapsed was not equal for all ten datasets because the total duration of each single run was not always the same. Also, the distance elapsed did not turn out to be a good criterion, since the GNSS module records data with a considerable deviation. So, another approach needed to be employed. The proposed method includes the following steps:

1) Organization of the latitude, longitude, and altitude data in matrices associated with each experiment,
2) Selection of one dataset (one route) as a reference dataset,
3) Detection of nearest positions in each of following experiments related to the reference dataset,
4) Evaluation of the average value of the nearest positions related to the reference one,
5) Determining the computed route as the new initial estimation (reference dataset)

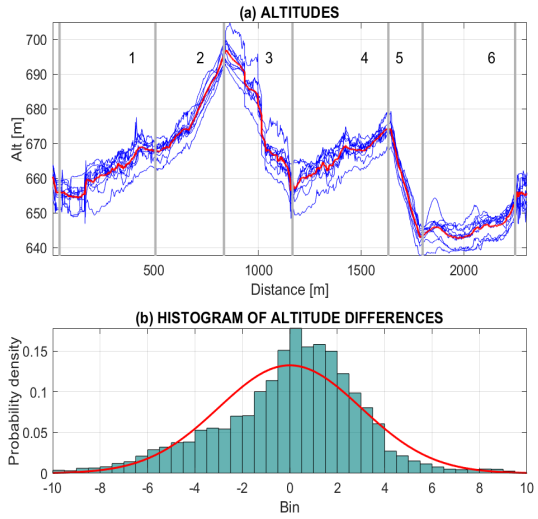

FIGURE 4. Altitude GNSS analysis presenting (a) altitude record during individual experiments, their mean value, and signal segments with different mean slopes, and (b) histogram of altitude differences.

6) Averaging of all datasets against the reference one equally as in previous items,
7) Iterative repetition of this process.

The proposed iterative process was verified by the Delaunay triangulation and two-dimensional interpolation. The selected route with the recorded longitude, latitude, and altitude was used as a reference. Altitude data from each other experiment were then interpolated into the same positions to enable the comparison and processing of its recalculated altitude data.

Figure 4(b) presents the analysis of observed altitude GNSS values during the set of all ten individual experiments. Differences between altitude values and their means evaluated for all experiments and all locations formed the set of 13,843 altitude data differences with their zero mean and standard deviation of 3 m. Owing to the range of altitude values of 60 meters, this accuracy was sufficient to separate signal segments with different slopes.

B. PHYSIOLOGICAL DATA ACQUISITION

Figure 5 presents the locations of the sensors on the body. The heart rate belt was located regularly on the chest and watches on the left wrist. The smartphone was located in vertical position with the display facing away from the back in its optimal position [4]. The mobile phone was used as the GNSS receiver, allowing the selection of the satellite system and recording of accelerometric data with the mobile Matlab for data acquisition. All physiological signals were recorded with their time stamps to allow their synchronization, resampling, and analysis.

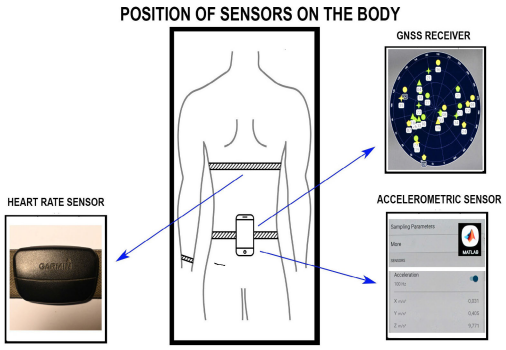

FIGURE 5. Position of sensors on the body including the heart rate sensors and the smartphone with the GNSS receiver and the acceleremetric sensor used with the mobile Matlab for data acquisition.

C. SIGNAL PROCESSING

The mathematical methods of data processing procedures are closely related to the properties of the sensors used for the data acquisition. However, in general, signal de-noising and the extraction of features in both the time and frequency domains create common problems in the preprocessing stage.

Each signal $\{x(n)\}_{n=0}^{N-1}$ was analysed at first to eliminate gross measurement errors and then smoothed by the low-pass finite impulse response (FIR) filter defined by the following relation:

$$y(n) = \sum_{k=0}^{M-1} b(k)\, x(n-k). \tag{1}$$

A selected normalised cutoff frequency f_c was used to evaluate a new sequence $\{y(n)\}$ for all values of $n = 0, 1, 2, \cdots, N-1$ and for filter coefficients $\{b(k)\}_{k=0}^{M-1}$. A polynomial approximation of the GNSS data was then applied to detect signal segments of similar route gradients and to find the regions with different mean slopes.

Accelerometric data recorded by the three-axis sensor formed three sequences $\{s_x(n),\ s_y(n),\ s_z(n)\}_{n=1}^{L}$, and their modulus,

$$s(n) = \sqrt{s_x(n)^2 + s_y(n)^2 + s_z(n)^2}, \tag{2}$$

for $n = 0, 1, \cdots, N-1$, was used for further processing. Signals were analysed in the frequency domain using the short-time discrete Fourier transform after the removal of the mean value $\bar{s} = mean(\{s(n)\}_{n=0}^{N-1})$ of the observed signal:

$$S(k) = \sum_{n=0}^{N-1} (s(n) - \bar{s})\, e^{-j\,k\,n\,2\,\pi/N}. \tag{3}$$

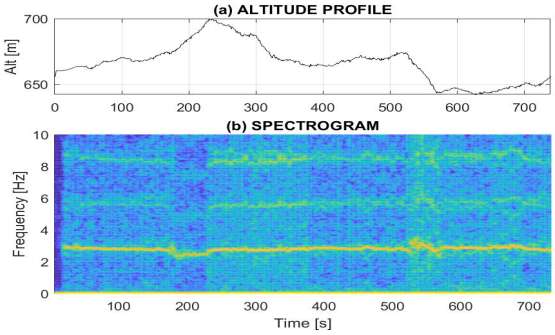

FIGURE 6. Accelerometric data analysis presenting (a) route profile associated with time stamps and (b) spectrogram of amplitudes of an accelerometric signal for a selected experiment.

Figure 6(b) presents the spectrogram of the accelerometric signal shown in Fig. 3(d) for a selected experiment 2303 m long (that lasted 740 s) evaluated with the window length of 1.5 s and the overlap of 50 % between contiguous sections.

The extraction of signal segments used for their subsequent classification was based upon the gradient of the altitude GNSS data recorded during each route to separate regions with different mean slopes.

D. FEATURE DESCRIPTION AND CLASSIFICATION

The classification of Q signal segments by a specific machine learning method requires the determination of the pattern and target matrices in most cases. All signal segments are associated with sets of column feature vectors $(p_1, p_2, \ldots, p_j, \ldots p_Q)$ and associated target classes $(T_1, T_2, \ldots, T_j, \ldots, T_Q)$ defined by a selected method (using the altitude gradient evaluated from the GNSS data in the given case). Each feature vector $\{p_j\}_{j=1}^{Q}$ includes R features $\{p(i,j)\}_{i=1}^{R}$ that form the feature matrix $P_{R,Q}$.

Signal features can be evaluated for data segments in the time, time–frequency or time-scale domains in most cases using either the discrete Fourier or wavelet transforms [38]. For accelerometric data, the frequency domain is selected in most cases. The use of spectral domain features requires the evaluation of the relative power E_w in the frequency band $B_w = \langle fc_1(w), fc_2(w)\rangle$:

$$E_w = \frac{\sum_{k\in\Phi_w} |S(k)|^2}{\sum_{k=0}^{L/2} |S(k)|^2}, \tag{4}$$

where Φ_w is the set of indices for the frequency components $f_k \in \langle fc_1(w), fc_2(w)\rangle$. In the given case, two frequency bands for the evaluation of the relative power were used: $B_1 = \langle 2.5, 5\rangle$ Hz and $B_2 = \langle 5, 10\rangle$ Hz to define the first (F1) and the second (F2) feature, respectively.

Commonly used algorithms for signal segment classification include the k-nearest neighbour (k-NN) algorithm with

its modifications, support vector machine, Bayesian, and neural network methods. To determine the ability of a predictive model to perform the classification during its practical implementation, the k-fold cross-validation method is often used. The cross-validation error is then evaluated as the fraction of the incorrectly determined target classes of data from the test set included in one of k folds of the original data set related to the number of pattern values. In the present paper, the leave-one-out method is used as a special case of k-fold cross-validation. The peculiarity of this method is that the number of folds k is the same as the number of data points in one data set. Each data point from the data set is extracted and classified by the rest of the data set.

The evaluation of the classification results was performed by the analysis of the multi-class receiver operating characteristic (ROC) to illustrate the performance of the classifier system. The ROC analysis was performed on the basis of a pairwise comparison of one class against all other classes. Common performance metrics include:

- Sensitivity of class k (True positive rate, recall) defined as a probability of correct classification of class k related to the number of instants belonging to class k:

$$TPR(k) = \frac{TP(k)}{TP(k) + FN(k)} \tag{5}$$

- Accuracy defined as a probability of global correct classification:

$$AC = \frac{\sum_k TP(k)}{\sum_k TP(k) + \sum_k FP(k)} \tag{6}$$

where $TP(k)$, $FN(k)$, and $FP(k)$ stand for the number of true positive, false negative, and false positive classifications of elements in class k.

III. RESULTS

The database of spectral measurements includes observations during 10 conditional runs on the route 2.303 km long in a real hilly environment with segments of the different mean slopes, as presented in Figs. 3 and 4. The mean time of running experiments was 798.2 s (with the standard deviation of 35.1 s). All running sessions were accomplished by a single person on the same route in similar weather condition to minimise data interruption. Sensors used [39] for data acquisition are summarized in Table 1.

TABLE 1. The list of devices and sensors used for monitoring of motion and data acquisition on the running route.

Device	*Sensors / Use*	*Software tools*
Mobile phone (iPhone 12 mini, 2021)	*GNSS, accelerometer*	*Mobile Matlab, export to *.csv file*
Heart Rate Belt (Suunto Smart, 2019)	*heart rate*	*Suunto application, export into *.gpx file*
Smart Watches (Suonto Spartan Sport, 2017)	*communication with mobile phone*	

The longitude and latitude geopositioning data recorded during each experiment were acquired by the satellite navigation network and recorded in the mobile Matlab environment. Their projection onto the geographical environment included

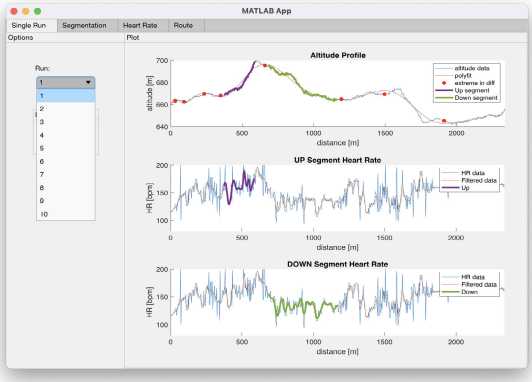

FIGURE 7. Graphical user interface used for the initial selected running session analysis.

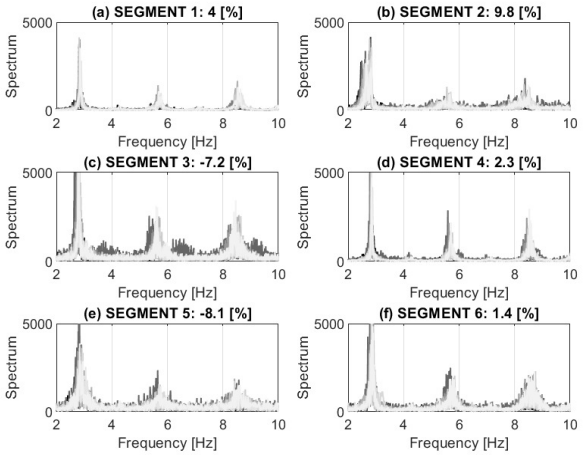

FIGURE 8. Spectral components of the accelerometric signal in the range of ⟨2, 10⟩ Hz in route segments with the different mean slopes for 10 separate runs.

the following commands and evaluations in the Matlab 2022b computational system:

```
\gg geoplot([Latitude],[Longitude],'.r')
\gg [LatLim,LongLim] = geolimits(gca);
\gg geobasemap steets
```

The red dots in Fig. 3 point to the route and the selection of the satellite geographical base map.

In order to simplify the visualisation of the data and the evaluation of the results, a graphical user interface (GUI) was created using the Matlab App Designer environment. The data were imported from the associated database and processed over several tabs.

Figure 7 presents the fundamental use of the GUI for visualization of the selected running session, showing the segmentation of the altitude route profile and the evolution of the heart rate in the selected segments related to ascending and descending motion. Further options enable displays of accelerometric signals, their spectral analysis, and distribution of selected features associated with different running patterns related to different route profiles.

TABLE 2. Values of the mean speed, mean heart rate *HR* [bpm], and mean percentage power of the accelerometric data in the frequency range of ⟨2.5, 5⟩ Hz (F1) and ⟨5, 10⟩ Hz (F2) with associated standard deviations (std) for segments with different slopes.

Segment	Slope		Speed [km/h]	HR [bpm]	F1 [%]	F2 [%]
1	4.0 %	mean	11.4	152	68.9	28.4
		std	1.7	10.4	7.8	8.9
2	9.8 %	mean	9.0	165	66.9	24.0
		std	3.1	13.9	5.5	5.9
3	-7.2 %	mean	13.6	133	59.2	35.6
		std	3.5	9.2	5.9	6.9
4	2.3 %	mean	11.6	144	66.1	31.5
		std	1.8	17.2	9.6	10.9
5	-8.1 %	mean	12.2	149	60.6	32.6
		std	2.6	15.5	6.3	7.7
6	1.4 %	mean	12.2	164	63.4	32.4
		std	1.9	3.9	8.5	9.9

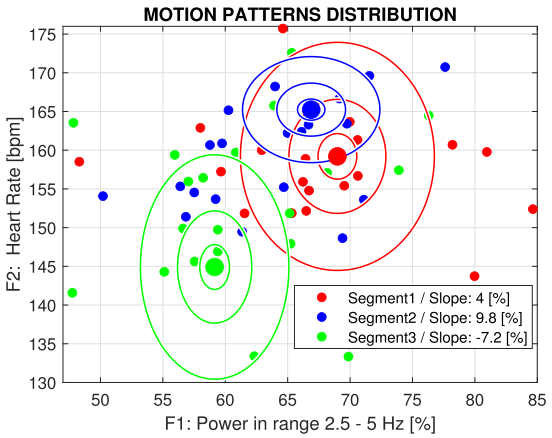

FIGURE 9. Distribution of features (heart rate and the mean power in the frequency range ⟨2.5, 5⟩ Hz) for running in three route segment with different mean slope and with means of each class and c multiples of their standard deviations for $c = 0.2$, 0.5, and 1.

The spectral components of the accelerometric signals specified by the gradient of altitude GNSS signals in segments with the different slope presented in Fig. 8 show their varying components. These properties motivated their use for feature extraction.

Table 2 presents the values of the mean speed, mean heart rate, and mean percentage power of the accelerometric data in the frequency ranges of ⟨2.5, 5⟩ Hz (F1) and ⟨5, 10⟩ Hz (F2) with associated standard deviations for segments with different slopes. The mean heart rate and the percentage power of the accelerometric signals in the first frequency band were used as two features for the classification of features associated with route segments of different slopes. Fig. 9 shows the distribution of these features in three route segments with means of each class and c multiples of their standard deviations for $c = 0.2$, 0.5, and 1.

Table 3 presents a comparison of classification of selected motion features for running on different slopes into three classes evaluated by a support vector machine (SVM), 5-nearest neighbour method (5NN), Bayesian method [40], and a two-layer neural network with the sigmoidal and softmax transfer functions using 10 neurons in its first layer. The pattern matrix was formed by features associated with three

TABLE 3. Classification results of running on different slopes performed by the support vector machine (SVM), 5-nearest neighbour (5NN), Bayesian, and two-layer neural network methods using two features specified as the power in the selected frequency accelerometric data band and the associated mean heart rate presenting the accuracy (AC), sensitivities (TPR(k)) of separate classes k, and the cross-validation errors (CV) calculated by the leave-one-out method.

Method	*AC [%]*	*TPR(1)*	*TPR(2)*	*TPR(3)*	*CV*
SVM Method	90	1.00	0.83	0.91	0.30
5NN Method	80	0.83	0.71	0.90	0.20
Bayesian Method	83.3	0.86	0.75	0.91	0.27
Neural Network	93.3	0.89	0.90	0.91	0.1

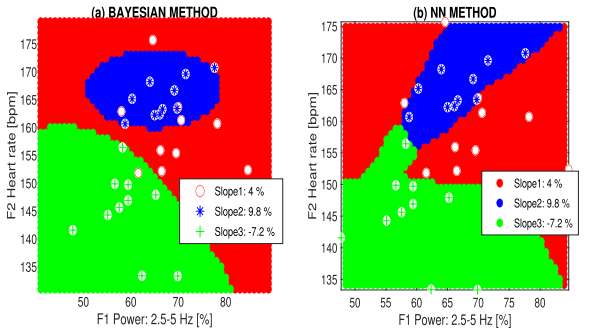

FIGURE 10. Results of the classification of selected motion features for running on different mean slopes (a) by the Bayesian method and (b) by the two-layer neural network.

first route segments and last three segments were used for verification. All associated algorithms [24] were created in the computational and visualization environment of MATLAB 2022b with the support of its toolboxes. The cross-validation errors were calculated by the leave-one-out method.

Figure 10 displays the results of classifying motion into three categories using the Bayesian method and a two-layer neural network. The results reveal that the clusters' locations and mean heart rate values vary depending on the segment slope.

IV. DISCUSSION

The paper is devoted to the study of the global navigation satellite system and selected wearable sensors for motion analysis. A set of 10 experiments was used for route segment analysis in the time and frequency domains. Analysis of GNSS data pointed to a standard deviation of altitude data of three meters for the given set of 13,843 satellite observations. Selected mathematical methods were used to classify route segments with the different mean slope.

The most important features for the classification of the route segments were based on signals recorded by the heart rate sensor and accelerometer inside a smartphone located in a selected body position. The heart rate and power of the accelerometric signals in selected frequency bands formed the most important features for further classification to separate clusters at different route segments. The classification accuracy reached 93.3% for the two-layer neural network with the cross-validation error by the leave-one-out method of 0.1.

TABLE 4. The summary of selected references and their keywords devoted to motion monitoring using GNSS systems combined with physiological data analysis published in 2020–2022.

Reference	*Keywords*	*Application*
Szot et al. [6]	GNSS receivers positioning accuracy	Motion analysis
Luteberget et al. [7]	Navigation systems; wearable sensors	Athlete monitoring
Sabry et al. [19]	Wearable devices; machine learning	Disease diagnosis; healthcare
Khundam et al. [36]	Virtual running; locomotion techniques	Physical fitness
Lou et al. [21]	Multi GNSS; ambiguity resolution	Precise orbit determination
Yu et al. [13]	Internet of Things	Exercise load monitoring
Charvatova et al. [41]	Motion features; neural networks	Cycling motion monitoring
This paper	GNSS signals; machine learning	Physiological data processing

Table 4 presents a very limited summary of selected references devoted to motion monitoring using GNSS systems, wearable sensors for physiological data acquisition, and machine learning methods for signal analysis published in 2020–2022. Interest in related methods is rapidly increasing due to the fast technological progress and their wide range of applications.

V. CONCLUSION

The paper presents possibilities of the motion monitoring during running experiments to classify the heart rate dynamics at different external conditions. A graphical user interface for the analysis of motion patterns acquired in real conditions was created and used for the visualization of the route segments, the analysis of the observed signals, and their segmentation and classification.

These results suggest that this method could help in identifying motion patterns based upon signals observed either in real conditions or in advanced virtual reality environments that can replace real situations. Future studies should focus on more complex computational methods and the use of sensor systems to monitor motion patterns, recognize motion disorders, and control mobile systems in engineering and biomedicine. The applications will include the use of more sophisticated sensors to study heart dynamics and monitor possible heart disorders. Further studies will explore the use of portable electrocardiographs to detect heart problems more accurately. All of these topics are closely related to the development of further mathematical methods, deep learning strategies, heart rate controllers, and augmented reality utilization.

REFERENCES

[1] W. Tao, T. Liu, R. Zheng, and H. Feng, "Gait analysis using wearable sensors," *Sensors*, vol. 12, no. 2, pp. 2255–2283, Feb. 2012.

[2] R. T. Li, S. R. Kling, M. J. Salata, S. A. Cupp, J. Sheehan, and J. E. Voos, "Wearable performance devices in sports medicine," *Sports Health, Multidisciplinary Approach*, vol. 8, no. 1, pp. 74–78, Jan. 2016.

[3] A. Prochazka, M. Schatz, O. Tupa, M. Yadollahi, O. Vysata, and M. Walls, "The MS Kinect image and depth sensors use for gait features detection," in *Proc. IEEE Int. Conf. Image Process. (ICIP)*, Oct. 2014, pp. 2271–2274.

[4] O. Dostál, A. Procházka, O. Vyšata, O. Ťupa, P. Cejnar, and M. Vališ, "Recognition of motion patterns using accelerometers for ataxic gait assessment," *Neural Comput. Appl.*, vol. 33, no. 7, pp. 2207–2215, Apr. 2021.

[5] X. Liu, S. Rajan, N. Ramasarma, P. Bonato, and S. I. Lee, "The use of a finger-worn accelerometer for monitoring of hand use in ambulatory settings," *IEEE J. Biomed. Health Informat.*, vol. 23, no. 2, pp. 599–606, Mar. 2019.

[6] T. Szot, C. Specht, P. S. Dabrowski, and M. Specht, "Comparative analysis of positioning accuracy of Garmin Forerunner wearable GNSS receivers in dynamic testing," *Measurement*, vol. 183, Oct. 2021, Art. no. 109846.

[7] L. S. Luteberget and M. Gilgien, "Validation methods for global and local positioning-based athlete monitoring systems in team sports: A scoping review," *BMJ Open Sport Exerc. Med.*, vol. 6, no. 1, Aug. 2020, Art. no. e000794.

[8] A. Jain and V. Kanhangad, "Human activity classification in smartphones using accelerometer and gyroscope sensors," *IEEE Sensors J.*, vol. 18, no. 3, pp. 1169–1177, Feb. 2018.

[9] M. del Rosario, S. Redmond, and N. Lovell, "Tracking the evolution of smartphone sensing for monitoring human movement," *Sensors*, vol. 15, no. 8, pp. 18901–18933, Jul. 2015.

[10] P. Silsupadol, K. Teja, and V. Lugade, "Reliability and validity of a smartphone-based assessment of gait parameters across walking speed and smartphone locations: Body, bag, belt, hand, and pocket," *Gait Posture*, vol. 58, pp. 516–522, Oct. 2017.

[11] B. Cvetković, R. Szeklicki, V. Janko, P. Lutomski, and M. Luštrek, "Real-time activity monitoring with a wristband and a smartphone," *Inf. Fusion*, vol. 43, pp. 77–93, Sep. 2018.

[12] G. M. Weiss, K. Yoneda, and T. Hayajneh, "Smartphone and smartwatch-based biometrics using activities of daily living," *IEEE Access*, vol. 7, pp. 133190–133202, 2019.

[13] Z. Yu, "Research on fitness movement monitoring system based on Internet of Things," *J. Healthcare Eng.*, vol. 2022, pp. 1–7, Mar. 2022.

[14] A. Procházka, S. Vaseghi, H. Charvátová, O. Ťupa, and O. Vyšata, "Cycling segments multimodal analysis and classification using neural networks," *Appl. Sci.*, vol. 7, no. 6, p. 581, Jun. 2017.

[15] O. Geman, S. Sanei, I. Chiuchisan, A. Graur, A. Prochazka, and O. Vysata, "Towards an inclusive Parkinson's screening system," in *Proc. 18th Int. Conf. Syst. Theory, Control Comput. (ICSTCC)*, Oct. 2014, pp. 475–481.

[16] S. Majumder and M. J. Deen, "Smartphone sensors for health monitoring and diagnosis," *Sensors*, vol. 19, no. 9, p. 2164, May 2019.

[17] S. O. Slim, A. Atia, M. M. A., and M.-S. M. Mostafa, "Survey on human activity recognition based on acceleration data," *Int. J. Adv. Comput. Sci. Appl.*, vol. 10, no. 3, pp. 84–98, 2019.

[18] A. Lucas, J. Hermiz, J. Labuzetta, Y. Arabadzhi, N. Karanjia, and V. Gilja, "Use of accelerometry for long term monitoring of stroke patients," *IEEE J. Transl. Eng. Health Med.*, vol. 7, pp. 1–10, 2019.

[19] F. Sabry, T. Eltaras, W. Labda, K. Alzoubi, and Q. Malluhi, "Machine learning for healthcare wearable devices: The big picture," *J. Healthcare Eng.*, vol. 2022, pp. 1–25, Apr. 2022.

[20] S. Jin, Q. Wang, and G. Dardanelli, "A review on multi-GNSS for Earth observation and emerging applications," *Remote Sens.*, vol. 14, no. 16, p. 3930, Aug. 2022.

[21] Y. Lou, X. Dai, X. Gong, C. Li, Y. Qing, Y. Liu, Y. Peng, and S. Gu, "A review of real-time multi-GNSS precise orbit determination based on the filter method," *Satell. Navigat.*, vol. 3, no. 1, pp. 1–15, Dec. 2022.

[22] D. Janos, P. Kuras, and Ł. Ortyl, "Evaluation of low-cost RTK GNSS receiver in motion under demanding conditions," *Measurement*, vol. 201, Sep. 2022, Art. no. 111647.

[23] R. Tamimi, "Relative Accuracy found within iPhone data collection," *Int. Arch. Photogramm., Remote Sens. Spatial Inf. Sci.*, vols. XLIII-B2-2022, pp. 303–308, May 2022.

[24] A. Procházka, O. Vyšata, and V. Mařík, "Integrating the role of computational intelligence and digital signal processing in education," *IEEE Signal Process. Mag.*, vol. 38, no. 3, pp. 154–162, May 2021.

[25] B. Langari, S. Vaseghi, A. Prochazka, B. Vaziri, and F. T. Aria, "Edge-guided image gap interpolation using multi-scale transformation," *IEEE Trans. Image Process.*, vol. 25, no. 9, pp. 4394–4405, Sep. 2016.

[26] B. Hofmann-Wellenhof, H. Lichtenegger, and E. Wasle, *GNSS Global Navigation Satellite Systems: GPS, GLONASS, Galileo, and More*. Austria, Vienna: Springer, 2007.

[27] J. Yu, X. Meng, B. Yan, B. Xu, Q. Fan, and Y. Xie, "Global navigation satellite system-based positioning technology for structural health monitoring: A review," *Struct. Control Health Monitor.*, vol. 27, no. 1, Jan. 2020, Art. no. e2467.

[28] H. Ye, L. Sheng, T. Gu, and Z. Huang, "SELoc: Collect your location data using only a barometer sensor," *IEEE Access*, vol. 7, pp. 88705–88717, 2019.

[29] K. A. Mackintosh, A. H. K. Montoye, K. A. Pfeiffer, and M. A. McNarry, "Investigating optimal accelerometer placement for energy expenditure prediction in children using a machine learning approach," *Physiolog. Meas.*, vol. 37, no. 10, pp. 1728–1740, Oct. 2016.

[30] A. Mannini and S. S. Intille, "Classifier personalization for activity recognition using wrist accelerometers," *IEEE J. Biomed. Health Informat.*, vol. 23, no. 4, pp. 1585–1594, Jul. 2019.

[31] H. Allahbakhshi, L. Conrow, B. Naimi, and R. Weibel, "Using accelerometer and GPS data for real-life physical activity type detection," *Sensors*, vol. 20, no. 3, p. 588, Jan. 2020.

[32] A. Prochazka, O. Dostal, P. Cejnar, H. I. Mohamed, Z. Pavelek, M. Valis, and O. Vysata, "Deep learning for accelerometric data assessment and ataxic gait monitoring," *IEEE Trans. Neural Syst. Rehabil. Eng.*, vol. 29, pp. 360–367, 2021.

[33] K. J. Hunt, R. Grunder, and A. Zahnd, "Identification and comparison of heart-rate dynamics during cycle ergometer and treadmill exercise," *PLoS ONE*, vol. 14, no. 8, Aug. 2019, Art. no. e0220826.

[34] H. Wang and K. J. Hunt, "Identification of heart rate dynamics during treadmill exercise: Comparison of first- and second-order models," *Biomed. Eng. OnLine*, vol. 20, no. 1, pp. 1–10, Dec. 2021.

[35] Y. Kong and K. H. Chon, "Heart rate tracking using a wearable photoplethysmographic sensor during treadmill exercise," *IEEE Access*, vol. 7, pp. 152421–152428, 2019.

[36] C. Khundam and F. Nöel, "A study of physical fitness and enjoyment on virtual running for exergames," *Int. J. Comput. Games Technol.*, vol. 2021, pp. 1–16, Apr. 2021.

[37] B. McIlroy, L. Passfield, H.-C. Holmberg, and B. Sperlich, "Virtual training of endurance cycling—A summary of strengths, weaknesses, opportunities and threats," *Frontiers Sports Act. Living*, vol. 3, Mar. 2021, Art. no. 631101.

[38] E. Jerhotová, J. Švihlík, and A. Procházka, *Biomedical Image Volumes Denoising Via the Wavelet Transform*. Rijeka, Croatia: InTech, 2011, pp. 435–458.

[39] J. P. Barrajón and A. F. S. Juan, "Validity and reliability of a smartphone accelerometer for measuring lift velocity in bench-press exercises," *Sustainability*, vol. 12, no. 6, p. 2312, Mar. 2020.

[40] A. Procházka, O. Vyšata, M. Vališ, O. Ťupa, M. Schätz, and V. Mařík, "Bayesian classification and analysis of gait disorders using image and depth sensors of Microsoft Kinect," *Digit. Signal Process.*, vol. 47, pp. 169–177, Dec. 2015.

[41] H. Charvatova, A. Prochazka, O. Vysata, C. P. Suarez-Araujo, and J. H. Smith, "Evaluation of accelerometric and cycling cadence data for motion monitoring," *IEEE Access*, vol. 9, pp. 129256–129263, 2021.

ALEŠ PROCHÁZKA (Life Senior Member, IEEE) received the Ph.D. degree, in 1983. He was appointed as a Professor of technical cybernetics with Czech Technical University (CTU) in Prague, in 2000. He is currently the Head of the Digital Signal and Image Processing Research Group, Department of Computing and Control Engineering, UCT Prague, and the Czech Institute of Informatics, Robotics and Cybernetics, CTU in Prague. His research interests include the mathematical methods of multidimensional data analysis, segmentation, feature extraction, classification, and modeling in biomedicine and engineering. He is a member of IET and EURASIP. He has served as an Associate Editor for *Signal, Image and Video Processing* journal (Springer-Verlag). He is a reviewer of different IEEE, Springer-Verlag, and Elsevier journals.

ALEXANDRA MOLČANOVÁ received the B.Sc. degree in physical and computational chemistry with the University of Chemistry and Technology Prague, Czech Republic, in 2022. She is currently a member of the Digital Signal and Image Processing Research Group, Department of Mathematics, Informatics and Cybernetics. Her research interests include information engineering, image processing, visualisation tools, computational methods of multidimensional data analysis, feature extraction, machine learning, classification, biomedicine, neurology, and physiological data processing.

HANA CHARVÁTOVÁ received the Ph.D. degree in chemistry and materials technology from the Faculty of Technology, Tomas Bata University (TBU) in Zlín, in 2007, with a focus on the technology of macromolecular substances. Currently, she is associated with the Centre for Security, Information and Advanced Technologies (CEBIA Tech), Faculty of Applied Informatics, TBU in Zlín. Her research interests include the modeling manufacturing processes of natural and synthetic polymers, the analysis of thermal processes in building technology, the studies of sensor system and wireless communication, signal processing for motion monitoring, and modeling engineering and information systems. She is oriented towards computational and visualization methods in thermographics, spatial modeling, and engineering. She serves as a reviewer for Springer-Verlag, Elsevier, Wiley, Taylor and Francis, and MDPI journals.

OANA GEMAN (Senior Member, IEEE) received the Ph.D. degree in electronics and telecommunication, in 2005. She is currently an Associate Professor with the Human and Health Development Department, Stefan cel Mare University of Suceava, Romania. Her current research interests include the non-invasive measurements of biomedical signals, wireless sensors, signal processing, artificial intelligence, nonlinear dynamics, stochastic networks, neuro-fuzzy methods, bioinformatics, biostatistics, biomedicine, the detection of neurological disorders, and rehabilitation. She has served as a member for the Technical Committees and the chair for several international conferences. She is a Reviewer of many journals, including IEEE TRANSACTIONS, IEEE ACCESS, IEEE INTERNET OF THINGS JOURNAL, *Sensors*, and *Symmetry*.

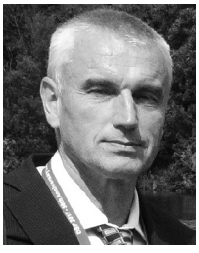

OLDŘICH VYŠATA (Member, IEEE) received the M.D. and Ph.D. degrees in technical cybernetics from the University of Chemistry and Technology (UCT) Prague, Czech Republic, in 1985 and 2011, respectively. He is currently a member of the Digital Signal and Image Processing Research Group at the Department of Mathematics, Informatics and Cybernetics, UCT Prague. He is also associated with the Neurological Department, University Hospital, Faculty of Medicine in Hradec Králové, Charles University, Czech Republic. His research interests include computational medicine, the analysis of motion disorders, and machine learning. He is a member of the European Neurological Society, the Czech Society of Clinical Neurophysiology, the Czech League Against Epilepsy, and the Czech Medical Association of J. E. Purkyně. He serves as a reviewer for different Springer-Verlag, Elsevier, and MDPI journals.